energies

MDPI

Article

Dynamic Rating Management of Overhead Transmission Lines Operating under Multiple Weather Conditions

Raquel Martinez [1,*], Mario Manana [1], Alberto Arroyo [1], Sergio Bustamante [1], Alberto Laso [1], Pablo Castro [1] and Rafael Minguez [2]

[1] Department of Electrical and Energy Engineering, University of Cantabria, Av. Los Castros s/n., 39005 Santander, Spain; mananam@unican.es (M.M.); arroyoa@unican.es (A.A.); bustamantes@unican.es (S.B.); alberto.laso@unican.es (A.L.); pablo.castro@unican.es (P.C.)

[2] Viesgo Distribution, S.L. C/ Isabel Torres 25, (PCTCAN), 39011 Santander, Spain; rafael.minguez@viesgo.com

* Correspondence: raquel.martinez@unican.es; Tel.: +34-942846518

Abstract: Integration of a large number of renewable systems produces line congestions, resulting in a problem for distribution companies, since the lines are not capable of transporting all the energy that is generated. Both environmental and economic constraints do not allow the building new lines to manage the energy from renewable sources, so the efforts have to focus on the existing facilities. Dynamic Rating Management (DRM) of power lines is one of the best options to achieve an increase in the capacity of the lines. The practical application of DRM, based on standards IEEE (Std.738, 2012) and CIGRE TB601 (Technical Brochure 601, 2014) , allows to find several deficiencies related to errors in estimations. These errors encourage the design of a procedure to obtain high accuracy ampacity values. In the case of this paper, two methodologies have been tested to reduce estimation errors. Both methodologies use the variation of the weather inputs. It is demonstrated that a reduction of the conductor temperature calculation error has been achieved and, consequently, a reduction of ampacity error.

Keywords: ampacity; conductor temperature; overhead transmission lines; weather parameters; real-time monitoring

Citation: Martinez, R.; Manana, M.; Arroyo, A.; Bustamante, S.; Laso, A.; Castro, P.; Minguez, R. Dynamic Rating Management of Overhead Transmission Lines Operating under Multiple Weather Conditions. *Energies* **2021**, *14*, 1136. https://doi.org/10.3390/en14041136

Academic Editors: Antonio Bracale, Pasquale De Falco and Andrea Michiorri

Received: 27 January 2021
Accepted: 11 February 2021
Published: 21 February 2021

1. Introduction

The integration of renewable energies into existing power lines has become a major difficulty to power distribution companies. The installation of a large number of renewable systems produces line congestions, resulting in a problem for distribution companies, since lines are not capable to transport all the energy generated. In addition, it results in a problem for generation companies, since they will be requested to limit production.

Increasing the capacity of overhead lines is an important research issue due to the great expansion of the renewable installations. Both environmental and economic constraints do not allow the construction of new lines to manage the energy from renewable sources, so the efforts have to focus on the existing facilities. Several techniques exist to increase line capacity: increase tension levels, increase the number of circuits, use of special conductors, and ampacity calculations (I_{max}). Ampacity means the maximum current a conductor can carry before sustaining deterioration. Procedures to calculate ampacity are divided by accuracy: use of deterministic meteorological conditions [1], use of probabilistic meteorological conditions [2], and real time monitoring (meteorological conditions, conductor temperature, line current, sag, and tilt) [3–5].

Monitoring of weather conditions and electric current of the overhead lines allows to estimate the capacity of the lines and the conductor temperature in a dynamic way. Dynamic Rating Management (DRM) of power lines is one of the best options to achieve an increase in the capacity of the lines [6]. Today, the development of this technique is enabling companies to operate in real time with higher capacities based on the real time

meteorological variables. These types of techniques can operate acting over two main values, conductor temperature (T_c) or ampacity (I_{max}). On one hand, DRM based on T_c allows to estimate the temperature of the line; operators can make decisions about whether increase or decrease the current of the lines with this temperature value. On the other hand, DRM based on I_{max} and the optimum loadability due to conductor thermal limit restrictions [7]. This information combined with other flexibility options increases the operational capability of the grid in several ways [8,9].

During the develop of different research projects with some of the leading electrical companies of Spain (DYNELEC: Dynamic Management in Lines, Fail Analysis and Quality of Supply in Distribution Viesgo Network (IPT-2011-1447-920000), SPADI: Predictive System for Dynamic Management of Overhead and Underground Power Lines (RETOS COLABORACIÓN RTC-2015-3795-3), and Development Model of Dynamic Capacity of Overhead Lines (FP7 EC-GA Nº 249812)), the authors found that the accuracy of the results in the the practical application of DRM was a weak point. In addition, in technical literature there are references about the problems with the accuracy of the DRM systems [9–12]. The practical application of DRM allows finding several deficiencies related to errors in T_c estimations, and consequently in I_{max} [13]. Therefore, the aim of this paper was to develop a methodology to increase of the dynamic rating methods.

2. Dynamic Rating Management (DRM) Using a Multiple Weather Station System

Existing dynamic rating models are mainly based on IEEE (Institute of Electrical and Electronics Engineers) 738 [14] and CIGRE (International Council on Large Electric Systems) TB601 [15] procedures. These procedures can be used to provide T_c and I_{max} using the same thermal model. In the case of T_c estimation, conductor parameters, weather conditions and current through the conductor are required, while, in I_{max} estimations, conductor parameters, weather conditions, and maximum temperature of the conductor are required ($T_{c_{max}}$).

First of all, it is raised the thermal balance equation:

$$Heat\ loss = Heat\ gain. \tag{1}$$

The thermal balance raised in IEEE 738 and in CIGRE TB601 provides calculations terms for all possible thermal flows as Joule heating, magnetic heating, solar heating, convective cooling, and radiative cooling. Magnetic heating is neglected or integrated as a coefficient. The thermal balance follows the next equation:

$$q_c + q_r = q_s + q_j, \tag{2}$$

where q_c is the cooling due to convection, q_r is the cooling due to the radiation to the surroundings, q_s is the heating due to the solar radiation, and q_j is the heating due to the Joule effect.

If the thermal inertia of the conductor is considered, the following dynamic thermal balance is used instead:

$$m \cdot c \frac{dT_c}{dt} + q_c + q_r = q_s + q_j, \tag{3}$$

where m is the mass per unit length, c the specific heat capacity, and T_c the theoretical conductor temperature.

Although both IEEE 738 and CIGRE TB601 use the same thermal balance equation, heat terms are obtained with different approaches. As a result, T_c and I_{max} calculations will be different using each of the procedures, and, hence, they will have unequal accuracies [16].

The accuracy of the estimations depends on several aspects, the most important are: errors arising from the estimations procedures, errors due to the sensors, and errors due to the spot measurements.

Weather conditions are very important inputs in both procedures; hence, accuracy of the results highly depend on the number and location of the spot measurements. For this

reason, it is important to define a multiple weather station system to monitor most of the line.

A generic i-th Weather Station WS^i can be modeled from a numerical point of view as a multi-sensor device. Considering that the time is sampled in slots, then, for each time slot $n \in \mathcal{N}$, the weather conditions of the generic WS^i can be defined as $\Omega_n^i = \{T_n^i, \omega_n^i, \phi_n^i, R_n^i\}$ $\forall n \in \mathcal{N}$, where T_n^i is the ambient temperature, ω_n^i is the wind speed, ϕ_n^i is the wind direction, and R_n^i is the solar radiation at sample n in weather station i.

Both IEEE 738 and CIGRE TB601 define a function $f_{IEEE} \equiv f_{CIGRE}$ that verifies f_{IEEE} and $f_{CIGRE} : \mathbb{R}^m \rightarrow \mathbb{R}$. Both procedures have two approaches represented in Figure 1, conductor temperature estimation T_c and ampacity estimation I_{max}, being $T_c = f(T, \omega, \phi, R, \zeta, I)$ and $I_{max} = f(T, \omega, \phi, R, \zeta, T_{c_{max}})$, where ζ is the angle of the line, I the real current of the line, and $T_{c_{max}}$ the maximum temperature of the conductor.

In the case of long lines or lines with heterogeneous weather conditions, procedures will consider multiple weather stations. Furthermore, a generic line is divided in t sections that are understood as the set of consecutive spans with the same direction. In this case, line conductor temperature verifies $T_c = max(f(\Omega_n^i, \zeta^t, I))$ and line ampacity $I_{max} = min(f(\Omega_n^i, \zeta^t, T_{c_{max}}))$ for all i and for all t, meaning the worst case.

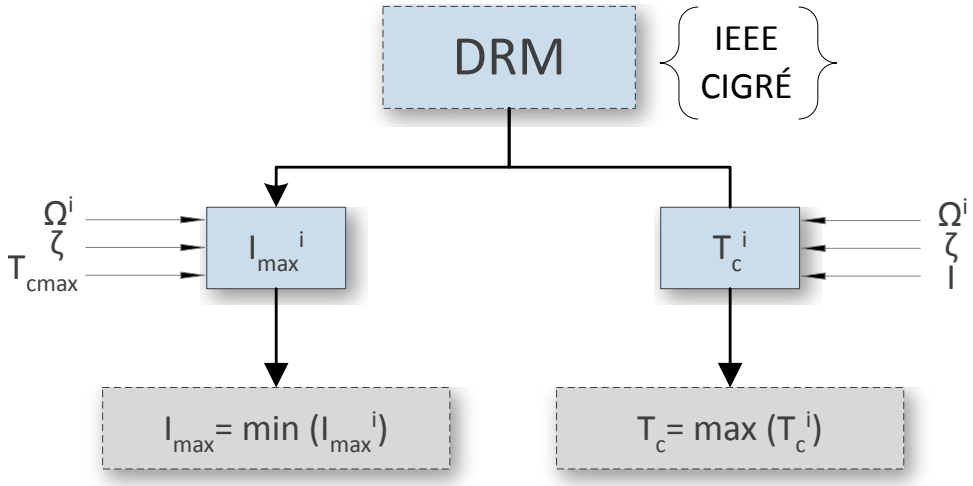

Figure 1. Dynamic Rating Management (DRM) system flowchart.

3. Practical Errors in Dynamic Rating Estimation in a Real Case

A practical scene is essential to put into practice the contributions raised in this article. A 220 kV line with estimated static ampacity of 889 A, located in the north of Spain, with a length of 30 km is selected for the study. Static ampacity is understood as the estimated maximum capacity of the conductor based on the R.D 223/2008 ITC-LAT 07 [17]. The line has a LA-455 conductor, 4 weather stations ($i = 4$) and is divided in 23 sections. Additionally, this line has a Distributed Temperature Sensor (DTS) that monitors approximately 10,200 points along the line with a resolution of 2 m. The sampling rate both DTS system and weather stations is 10 min, and an historic data of 3 years has been used. Due to this sampling rate, the ampacity and conductor temperature will calculated every 10 min. This system allows for the comparison of estimated and measured conductor temperature.

Practical use of IEEE 738 and CIGRE TB601 procedures in real lines allows to obtain much information about results of T_c and I_{max}. To create a robust and efficient system, it is necessary to verify the accuracy of results. It is important to know that it is not possible to directly determine the accuracy of the ampacity calculation, since ampacity is a non-measurable variable. For this reason, it is not possible to determine the accuracy of this calculation. Due to the similarity of ampacity and conductor temperature procedures, the accuracy of the calculations of ampacity can be estimated through the accuracy of conductor temperature procedure, since temperature can be measured.

Accuracy of the procedures is defined as:

$$\varepsilon_{T_c} = T_c^{DTS} - T_c, \tag{4}$$

where ε_{T_c} represents the error in T_c estimations, and T_c^{DTS} represents the measured conductor temperature.

In the real case studied, errors in T_c calculations using CIGRE TB601 are represented in Figure 2. It is observed that, in most cases, errors are mainly between -5 and 5 °C with a maximum of 20 °C. The Root Mean Squared Error (RMSE) of the calculation is 2.28 °C. These errors in temperature calculations have their origin in different issues, such as errors in procedures, in sensors, and by the use of spot measurement.

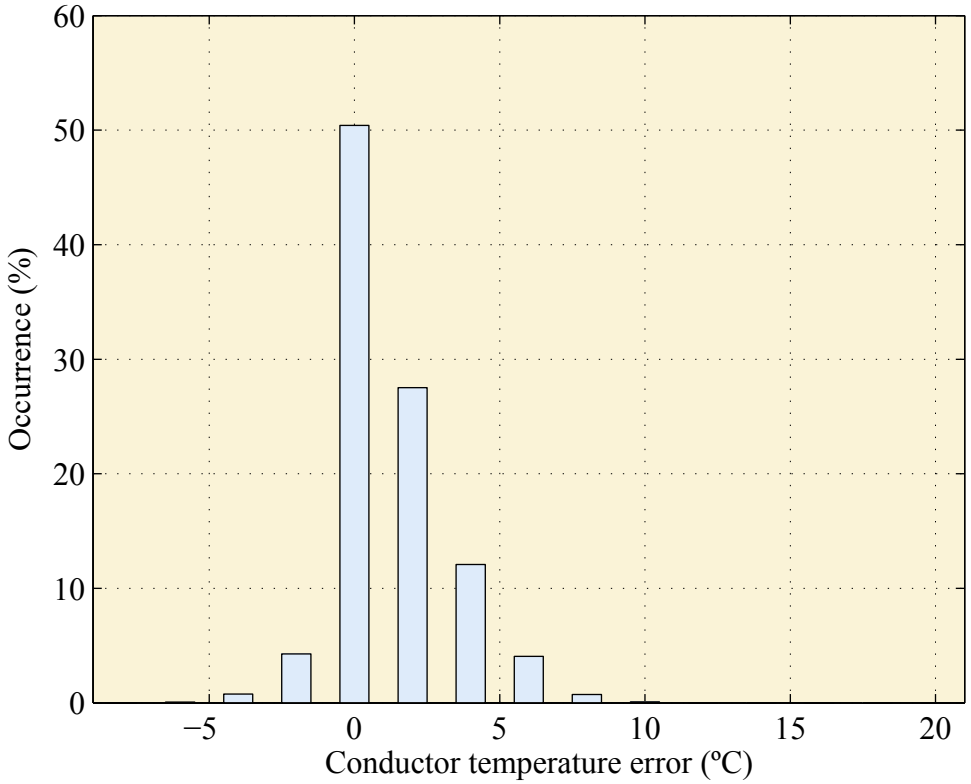

Figure 2. Error in conductor temperature (T_c) calculation using CIGRE TB601.

3.1. Errors due to Procedures IEEE (Std.738, 2012) and CIGRE TB601 (Technical Brochure 601, 2014)

Any theoretical model has a lack of accuracy in its equations due to the difficulty of matching the theoretical behavior of the equations with the real behavior of the system. In this case, it is necessary to assess the accuracy of the procedures.

Although these Standards have conceptualy equivalent procedures, the results of both are usually different. $T_c^{IEEE} \neq T_c^{CIGRE}$ and $I_{max}^{IEEE} \neq I_{max}^{CIGRE}$ since these procedures use different numerical approaches. Consequently, one of the procedures will be more appropriate depending on the case.

There are several factors in the procedures that increase errors. Firstly, both procedures allow calculations in two main states. It is possible to obtain T_c ans I_{max} in steady and unsteady state, defined in Equations (2) and (3), respectively. In practice, unsteady state obtains better results than steady state [18]. The unsteady state model obtains smoother curves with fewer differences with the measured temperature.

Secondly, both Standards use conductor and line parameters as inputs. On occasion, some of these parameters, such as emisivity and absortivity, are significant in calculations. However, there is no easy way to measure these quantities accurately. In CIGRE TB299 [19], values for these parameters are recommended.

Thirdly, both Standards calculate solar radiation heating (q_s) with theoretical approaches, obtaining solar radiation values that are more conservative than real ones. In Reference [18], the conductor temperature estimation with IEEE 738 and CIGRE TB601 and the measured temperature are compared. In addition, conductor temperature calculations with estimated solar radiation and with measured solar radiation are compared. It is observed that, focusing on a single day, with estimated radiation, deviations higher than 5 °C are presented in 15% of the samples, while, with measured radiation, this percentage decreases to 5%.

Fourthly, other weather parameters, different from mentioned, produce refrigeration or heating in the conductor. IEEE 738 and CIGRE TB601 do not take rain into account, being an important parameter for the refrigeration of the conductor [1,20]. In this case, measured conductor temperature will be lower than estimated conductor temperature during rainy periods.

Finally, in Reference [16], the relationship between errors in estimated conductor temperature and wind speed has been represented, reaching the conclusion that higher conductor temperature deviations occur during lower wind speed periods.

In conclusion, due to all of these factors, errors in IEEE 738 and CIGRE TB601 can reach high values.

3.2. Errors in Sensors

Weather conditions are one of the more significant inputs of the conductor temperature and ampacity calculations. IEEE 738 [14] and CIGRE TB601 [15] use, mainly, wind speed, wind direction, and ambient temperature. Furthermore, solar radiation measurements are necessary to obtain reasonable results based on Reference [18]. An anemometer, a wind vane, a thermometer, and a pyrometer are the sensors used to provide data to the procedures. In CIGRE TB299 [19], recommended values of accuracy to each sensor are provided. In ambient temperature case, a minimum accuracy of 1 °C is recommended. Regarding wind speed, a start and stall speed of no more than 0.5 m/s is raised. In general, sensors have their own accuracy, so the measurement errors produced in the sensors are transferred to the conductor temperature and ampacity estimations, shown in Equations (5)–(7).

$$\Omega_n^i = \Omega_{r,n}^i + \varepsilon_\Omega^i = \{T_{r,n}^i + \varepsilon_T^i,\ \omega_{r,n}^i + \varepsilon_\omega^i,\ \phi_{r,n}^i + \varepsilon_\phi^i,\ R_{r,n}^i + \varepsilon_R^i\}, \tag{5}$$

$$T_{cn}^i = T_{cr,n}^i + \varepsilon_{Tc}^i = f(\Omega_{r,n}^i + \varepsilon_\Omega^i,\ \zeta^t,\ I), \tag{6}$$

$$I_{max}{}_n^i = I_{max}{}_{r,n}^i + \varepsilon_{I_{max}}^i = f(\Omega_{r,n}^i + \varepsilon_\Omega^i,\ \zeta^t,\ T_{c_{max}}), \tag{7}$$

where the subscript r represents the real measurement, and ε_Ω is the error in weather conditions that is divided in; error of ambient temperature (ε_T), error of wind speed (ε_Ω), error of wind direction (ε_ϕ), and error of solar radiation (ε_R); and $\varepsilon_{I_{max}}$ represents error in ampacity.

It has been demonstrated, in a practical way, that errors of 0.5 m/s in wind measurements produce significant errors in ampacity and conductor temperature calculations [21]. In addition to weather conditions, conductor current is an important variable in conductor temperature calculation, but it is not included in the errors section due to the high accuracy of existing current sensors.

An example of the sensitivity of the procedures to the errors in sensors is in Reference [18]. Cup anemometers are compared with ultrasonic anemometers in Reference [18], and the main conclusion is that the use of cup anemometers instead of ultrasonic ones have an important impact in ampacity calculations at very low wind speeds. IEEE 738 and CIGRE TB601 recommend in their guides the use of ultrasonic anemometers.

Another example is provided in Reference [22]. In this paper, the differences between the use of measured solar radiation and estimated solar radiation are analyzed. Lower mean squared errors are obtained with measured solar radiation than with estimated solar

radiation. In addition, this paper concludes that differences increase when the sun rises, reaching errors up to 15 °C.

This type of error is analyzed with historical data of spring and summer of the studied line.

All sensors have their own errors, but, in some of them, it is difficult to know if the data is erroneous. In the case of wind speed, the high variability of its values make it difficult to find errors. In the case of ambient temperature, depending on the geographic situation, it is possible to find out off the normal range for all the WS.

In Figure 3, a box-plot with ambient temperature data is shown for all WS^i. In this box-plot, median, 25th, and 75th percentiles, maximum, minimum, and outliers are plotted. It is observed that, in the case of WS^1, there are a lot of outliers, reaching values of ambient temperature close to 50 °C, obviously erroneous. This indicates that WS^1 provides wrong data, so it will produce incorrect ampacity results due to errors in sensors. This wrong data is also observed in Figure 4. The consequences of this type of wrong data is that, with high ambient temperature, the ampacity can reach the lowest value of the line, and, consequently, it will assume this wrong value as ampacity of the whole line.

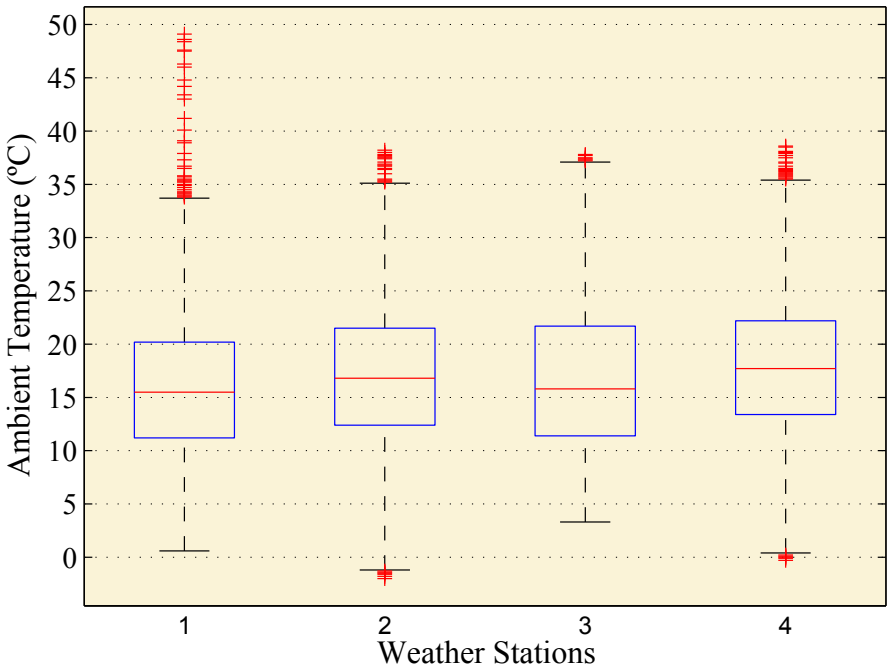

Figure 3. Box plot of ambient temperature for all weather stations along the line.

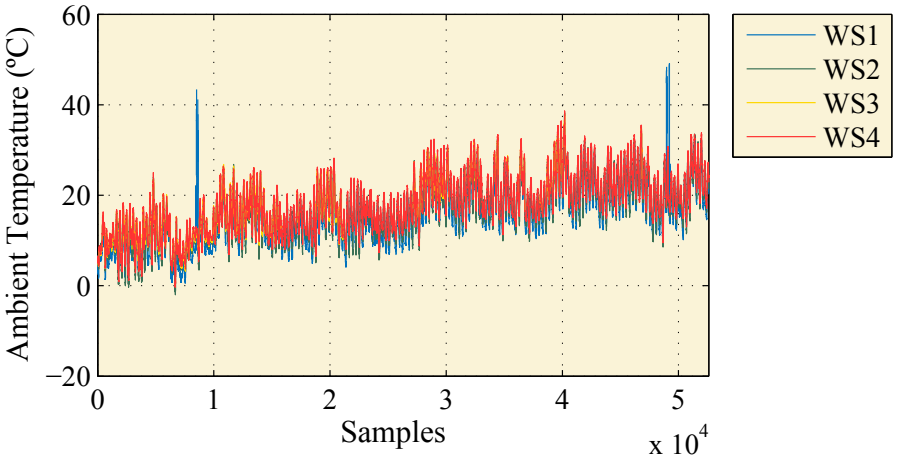

Figure 4. Evolution of ambient temperature with time.

In the case of solar radiation, it is easy to find wrong data if values at night are not zero or are much higher than normal values of the geographical zone. In the real case of this paper, there have been no sensor failures.

3.3. Errors due to the Use of Spot Measurements in a Long Line

Overhead lines have, usually, lengths from few to hundreds of kilometers. Due to these long distances, weather conditions can vary considerably along the line. Since it is not possible to monitor the weather conditions in a continuous way, it is necessary to install several weather stations. The number of the weather stations depends on the length of the line and the climatic and orographic characteristics of the zone. Overhead lines with long lengths or with different refrigeration characteristic along the line need more weather stations than short lines or lines with uniform atmospheric characteristics. To decide the number of weather stations, a complete statistical study of the climatology of the zone will be necessary.

In Figure 5, a theoretical line is represented. This line has m electric towers, t sections, and i weather stations. Section parameter, set of consecutive spans with the same direction, is important for the climatological study since spans with same direction will have equal attack angle of wind.

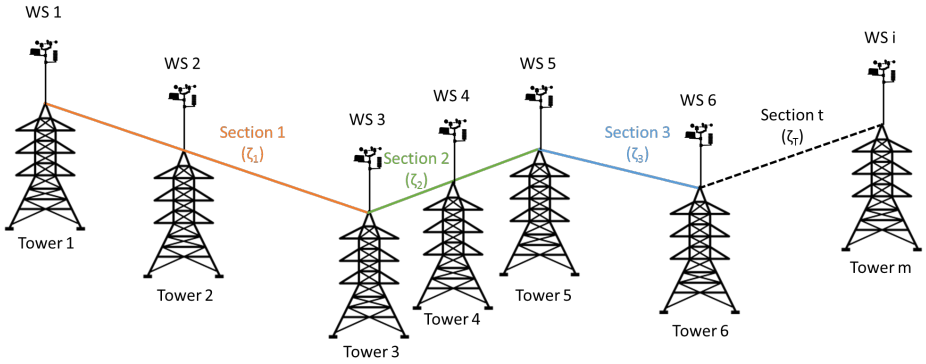

Figure 5. Parts of a theoretical line.

The maximum physically possible resolution system of weather stations is a system with one weather station in each tower ($m = i$). In this case, conductor temperature and ampacity in one tower will be:

$$T_{cn}^{i}(m) = f(\Omega_n^i, \zeta^t, I), \tag{8}$$

$$I_{max}{}_n^{i}(m) = f(\Omega_n^i, \zeta^t, T_{c_{max}}). \tag{9}$$

A system with less resolution would be the installation of one weather station per section ($t = i$). The solution adopted in the studied case is the installation of several weather stations according to a climatic study of the zone. In this case, it is necessary to define the area of influence of each weather station. These areas are defined in the climatic study. Due to this approach, several towers will be monitored with the same weather station depending on the influence area. An influence area can be large or can be affected by very different weather conditions, so it is possible that points within the same influence area have weather conditions quite different from those measured by the corresponding WS. Because of this, ampacity is obtained with Equation (9), and conductor temperature with Equation (8), for all m within influence area of WS^i.

As an example, Figure 6 represents a theoretical disposition of weather stations with less than ideal resolution.

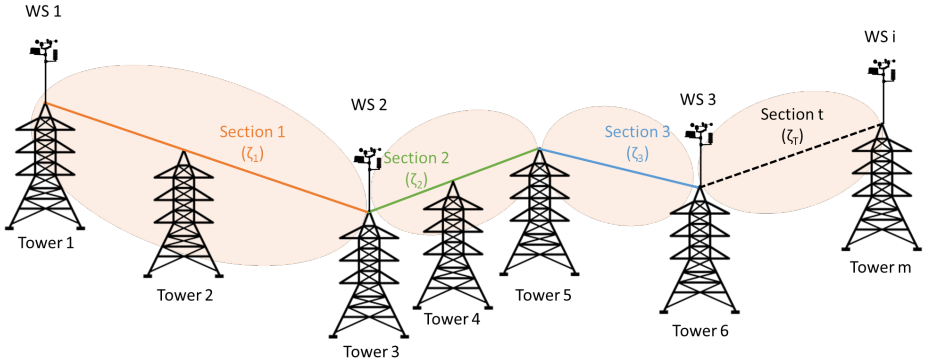

Figure 6. Parts of a theoretical line with less resolution.

In this case, conductor temperature and ampacity in tower 2 would be:

$$T_{c_n}^1(2) = f(\Omega_n^1, \zeta^1, I), \tag{10}$$

$$I_{max_n}^1(2) = f(\Omega_n^1, \zeta^1, T_{c_{max}}). \tag{11}$$

This calculation involves an error due to spot measuring since the weather conditions in tower 2 are different than the conditions of weather station 1 located in tower 1. On a comparison with the real value of an ideal system with infinite resolution:

$$T_{c_{r,n}}(2) = f(\Omega_n^2, \zeta^1, I), \tag{12}$$

$$I_{max_{r,n}}(2) = f(\Omega_n^2, \zeta^1, T_{c_{max}}), \tag{13}$$

$$T_{c_{r,n}}(2) \neq T_{c_n}^1(2), \tag{14}$$

$$I_{max_{r,n}}(2) \neq I_{max_n}^1(2). \tag{15}$$

So, finally, in a system with spot measurement, ampacity and conductor temperature can be represented as:

$$T_{c_n}^i = T_{c_{r,n}}(m) + \varepsilon_{T_c} = f(\Omega_n^i, \zeta^t, I), \tag{16}$$

for all m within influence area of WS^i.

$$I_{max_n}^i(m) = I_{max_{r,n}}(m) + \varepsilon_{I_{max}} = f(\Omega_n^i, \zeta^t, T_{c_{max}}), \tag{17}$$

for all m within influence area of WS^i.

The differences between weather conditions along the line produce T_c and I_{max} results that vary, widely on occasions. In addition to the variability of the weather conditions, conductor characteristics may change due to aging, joints, altitude, angle, etc.

In order to show these type of errors, Figure 7 represents the variability of the weather conditions along the line through a box plot with the differences between each weather station.

Maximum values of absolute median differences are in WS^{1-3}, WS^{3-4}. Median differences in WS^{1-2}, WS^{1-3}, WS^{1-4}, and WS^{2-3} are negative, while median differences in WS^{2-4} and WS^{3-4} are positive. All this shows that WS^1 and WS^4, which are placed in the ends of the line, usually obtain the lowest values of wind speed. In general terms, variability of wind speed along the line is significant, so the accuracy of the procedure is highly dependent on the number of measuring spots.

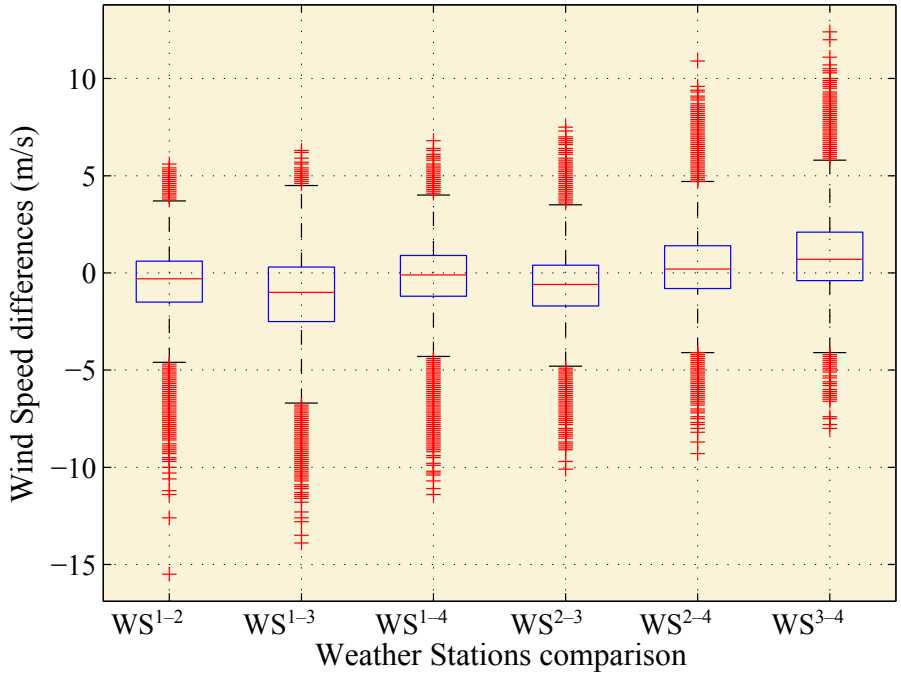

Figure 7. Box plots of wind speed differences between weather stations.

In Figure 8, it is clear that there are more differences between ambient temperatures of WS^1 and the others. So, it can be said that WS^1 obtains lower ambient temperature values than the others. Other stations apart from WS^1 have a less pronounced variability.

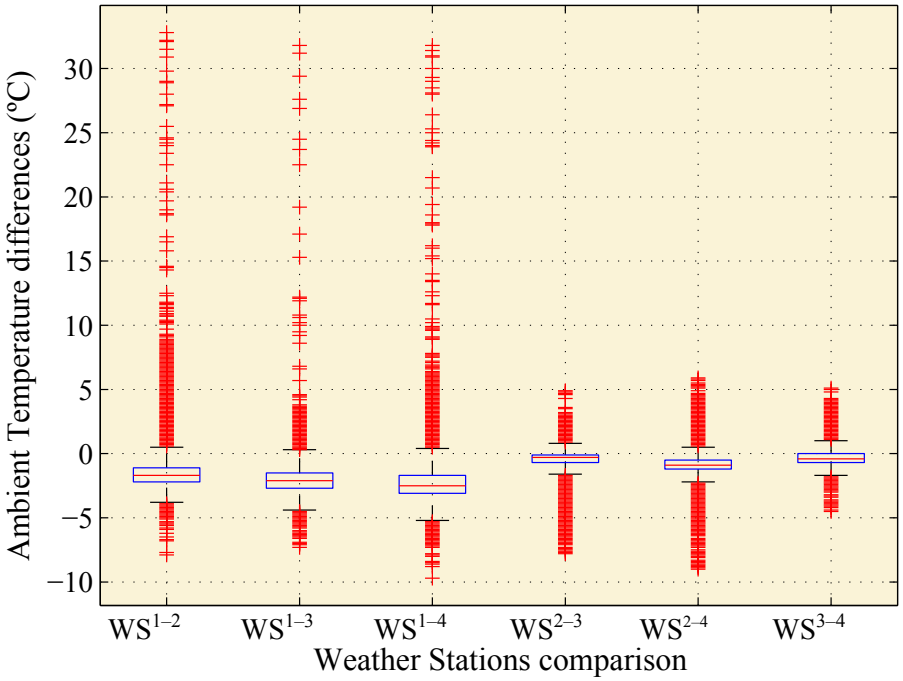

Figure 8. Box plots of ambient temperature differences between weather stations.

Finally, in Figure 9, the same as in ambient temperature occurs in solar radiation. WS^1 obtains lower values than the others. In general, it is shown that the variability in the case of solar radiation is very small.

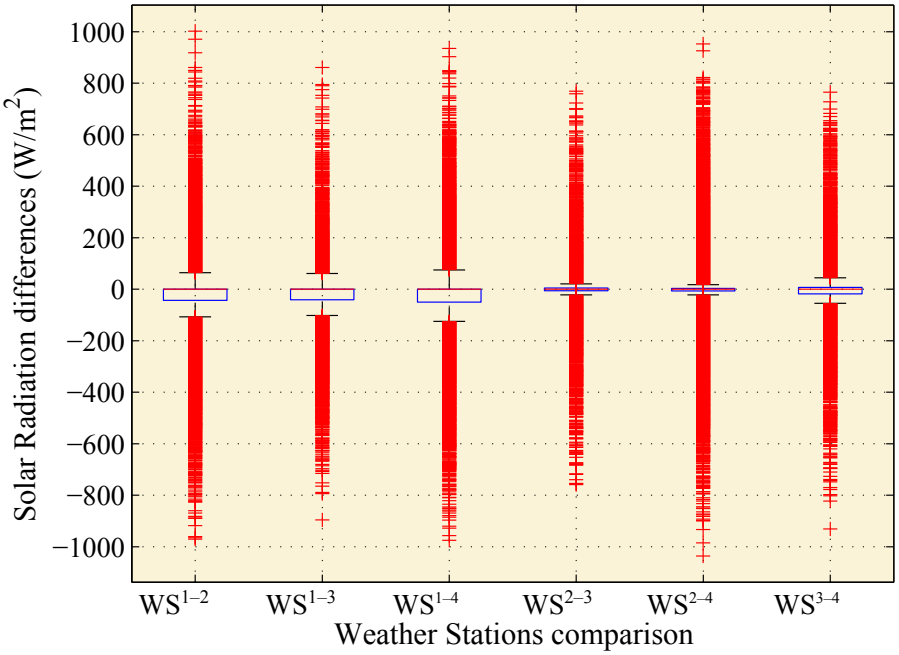

Figure 9. Box plots of solar radiation differences between weather stations.

The most important conclusion achieved with this study is that, due to the significant variability of wind speed, T_c or I_{max} results will be very affected by the number of measuring points, especially if weather stations are not placed in critical points.

Consequently, although the previous climatic study locates the estimated critical zone, no monitored critical points can exist. In this way, I_{max} and T_c results can be erroneous due to the use of spot measurements.

Conductor temperature differences can be observed in Figure 10. In this figure, conductor temperature along the line in one measurement interval n is represented. The white line represents the conductor temperature average for each section, red rectangle represents, in x axe, the start and the end of the section, and, in y axe, the maximum and the minimum value of all monitored points of the section. The blue line represents the conductor temperature measurements of the approximately 10,200 points of DTS system.

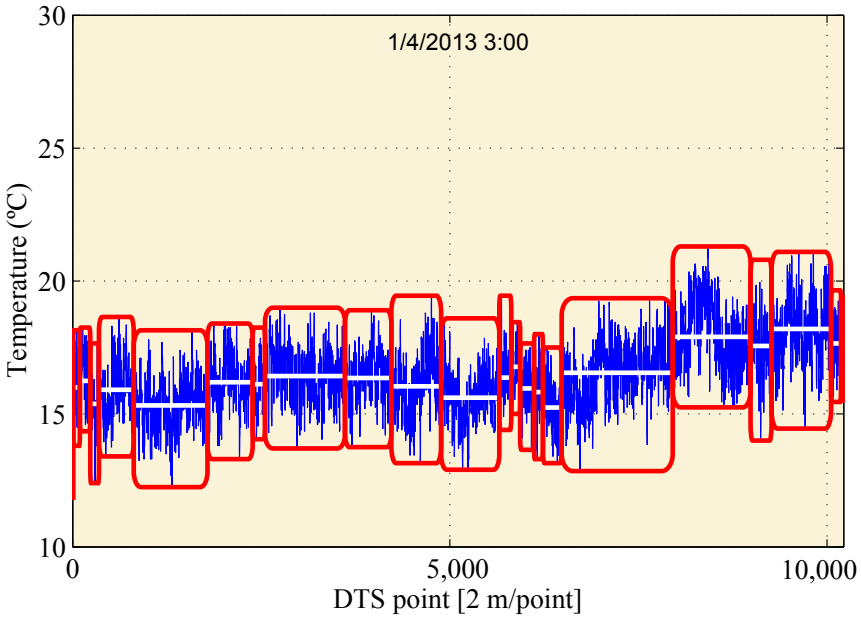

Figure 10. Evolution of conductor temperature along the line in a specific date.

It is observed that along the line, even within a section, conductor temperature values vary widely. For example, in the first part of the line, average value of conductor temperature vary little between consecutive sections, while, in the second part, average values are more variables.

This figure confirms that accuracy in the conductor temperature or ampacity calculation will depend on the number of weather stations installed.

The errors described in the previous section produce low accuracy results in the I_{max} and T_c calculations. In order to develop a proper DRM system, it is necessary to implement a procedure to reduce errors in I_{max} results.

Methodology to the improvement of the accuracy of ampacity calculations defines a method to adjust the results changing weather inputs. Currently, ampacity calculation is made with errors, where:

$$I_{max}{}_n^i(m) = I_{max}{}_{r,n}(m) + \varepsilon_{I_{max}} = f(\Omega_{r,n}(m) + \varepsilon_\Omega). \tag{18}$$

And the ideal aim of this paper is to obtain a calculation without errors, where:

$$I_{max}{}_n^i(m) = I_{max}{}_{r,n}(m) = f(\Omega_n^i + \triangle\Omega_n^i) = f(\Omega_{r,n}(m)). \tag{19}$$

4. Methodology

Once the existence of errors due to procedures, sensors, and the use of spot measurements has been demonstrated, it is important to define the methodology to reduce these errors.

This new algorithm is based on the similarity between ampacity and conductor temperature estimation. Conductor temperature, in this new approach, is monitored through DTS system, so it is possible to compare, for each instant, the measured value and the estimated one. Depending on the value of this comparison, the procedure changes the weather inputs until measured and estimated conductor temperature match. Once conductor temperature has been corrected, new meteorological values, known as effective values ($\Omega_{ef} = \{T_{ef}, \omega_{\perp_{ef}}, R_{ef}\}$), are used as inputs of the ampacity algorithm, achieving a more real ampacity value. Two approaches are applied in the search for meteorological effective values, an iteration method and a procedure based on Monte Carlo.

4.1. Iteration Method

In the iteration method, meteorological inputs are modified in order of significance in the conductor temperature estimation algorithm. The order of modification is first perpendicular wind ($\omega_\perp$), second ambient temperature (T), and, finally, solar radiation (R). Perpendicular wind is understood as a wind perpendicular to the line direction that provides the same refrigeration as the measured wind ($\omega_\perp = f(\Omega, \phi, \zeta)$) based on the equations raised by Morgan in Reference [23]. The increment of variation of each meteorological variable ($\Delta\Omega = \{\Delta T, \Delta\omega_\perp, \Delta R\}$) depends, in each iteration, on the difference between measured and estimated conductor temperature (er). The ranges of variations ($[T_{min}, T_{max}], [\omega_{\perp_{min}}, \omega_{\perp_{max}}], [R_{min}, R_{max}]$) are established according to statistical studies of the historical weather data of the zone.

The iteration method starts with the calculation of the conductor temperature with measured weather conditions. If the conductor temperature estimation is not in the range $[-er, er]$, meteorological values will be changed, while, if conductor temperature estimation is in the range $[-er, er]$, meteorological values are the final parameters (effective parameters) to calculate $I_{max_{ef}}$.

In the case of the conductor temperature estimation not being in the range $[-er, er]$, firstly, perpendicular wind is varied, increasing it if measured conductor temperature is lower than estimated and reducing it in the opposite case ($\omega_\perp(k) = \omega_\perp(k-1) + \Delta\omega_\perp(k)$), being k the number of iteration. When the effective wind value reaches the limit established ($[\omega_{\perp_{min}}, \omega_{\perp_{max}}]$) , it is fixed as the limit value. When this occurs, ambient temperature begins to be iterated, increasing it if measured conductor temperature is higher than

estimated and reducing it in the opposite case ($T(k) = T(k-1) + \Delta T(k)$). In the same way as perpendicular wind, when ambient temperature value reaches the established limit ($[T_{min}, T_{max}]$), it is fixed as the limit value. Finally, solar radiation is changed, increasing it if measured conductor temperature is higher than estimated and reducing it in the opposite case ($R(k) = R(k-1) + \Delta R(k)$). If solar radiation reaches the established limit ($[R_{min}, R_{max}]$) and estimated conductor temperature does not match with the measured one, it is considered that the method does not converge.

In the case convergence is achieved, the effective meteorological values will be the inputs of the ampacity model. Figure 11 summarizes the proposed methodology.

4.2. Monte Carlo Method

Monte Carlo is a non-deterministic method used to model complex mathematical expressions. This method provides approximate solutions using a sample of the total of the calculations in base on pseudo-random samples. In the case of this paper, Monte Carlo method is employed to obtain successive pseudo-random meteorological samples, among all the possible values. The pseudo-random samples are based on the distribution function of each parameter to give a physical base to the randomness. Distribution functions of ambient temperature, perpendicular wind, and solar radiation are estimated with historical values from a established time (7 days). This method is suggested by the necessity to perform the calculation of effective variables with a physical base. In the iteration case, limits of variation of each meteorological variable are established, but, in certain scenarios, effective meteorological results are not realistic. These unrealistic values can appear because of several reasons but are mainly due to errors in the procedure, in the measurement of the weather conditions, or by the use of spot measurements. These errors make the algorithm to introduce huge changes in the weather conditions to achieve values of measured conductor temperature. For this reason, in some cases, effective meteorological results are not realistic. In the case of Monte Carlo method, the effective meteorological values will always be within the distribution function of the preceding 7 days. An example of distribution function and cumulative distribution function for the meteorological variables is represented in Figures 12–14.

The calculation of effective parameters, with Monte Carlo method, starts with the calculation of T_c with the measured meteorological variables. If the error between the calculated T_c and the measured T_c by the DTS system is higher than an established error, the Monte Carlo method is applied. The first step in this method is to generate a pseudo-random number between 0 and 1. This value represents the occurrence in the cumulative distribution function of ambient temperature, perpendicular wind, and solar radiation. Therefore, a value of ambient temperature, perpendicular wind, and solar radiation will correspond with the pseudo-random occurrence value. These values are used as meteorological input in the temperature calculation algorithm. This will iterate until the error between the calculated T_c and the measured T_c by the DTS system is lower than established one or the Monte Carlo iteration limit is reached. A distribution with 7 previous days of historical data is obtained every instant of T_c and ampacity calculation. Figure 15 shows the flow diagram of the Monte Carlo method.

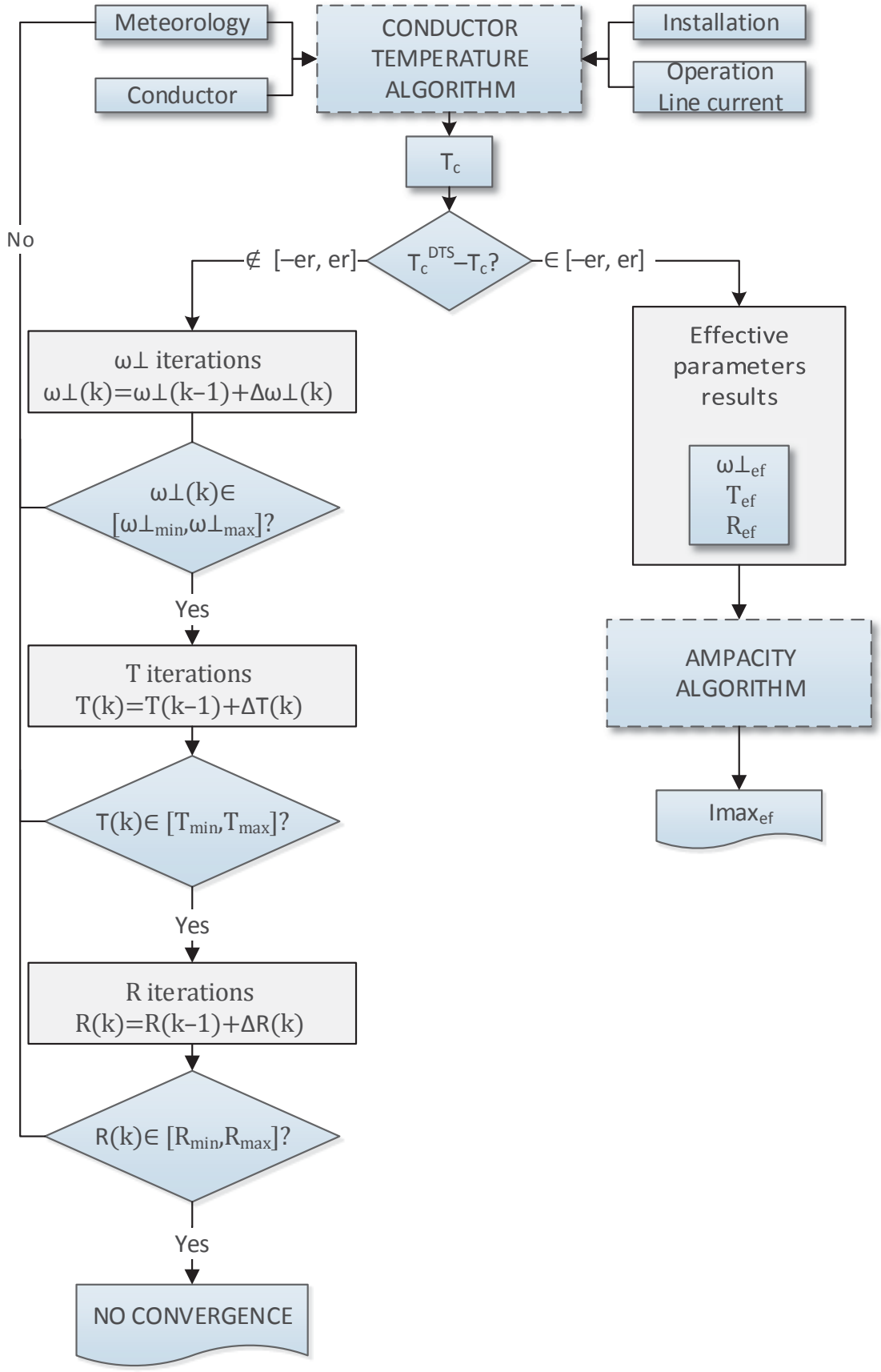

Figure 11. Iteration method flow diagram.

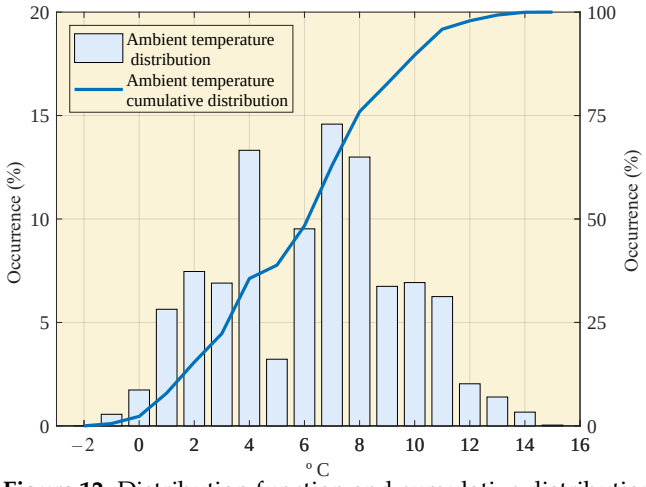

Figure 12. Distribution function and cumulative distribution function of ambient temperature for 7 days.

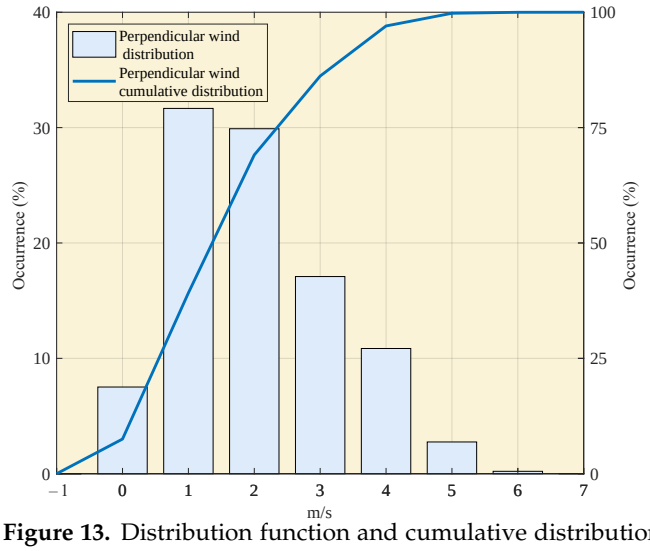

Figure 13. Distribution function and cumulative distribution function of perpendicular wind for 7 days.

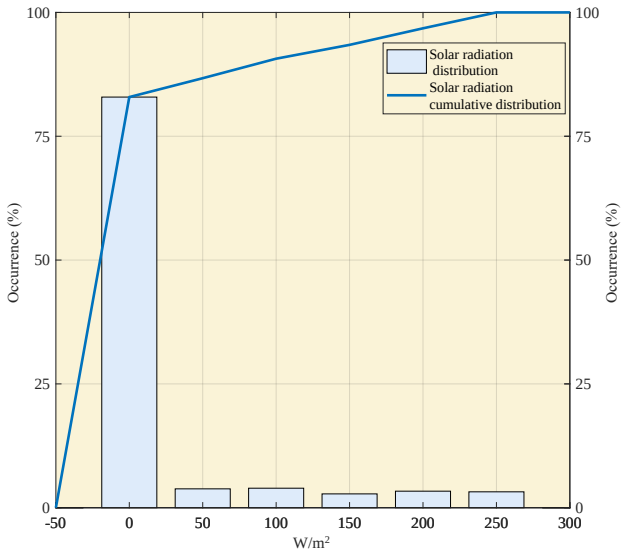

Figure 14. Distribution function and cumulative distribution function of solar radiation for 7 days.

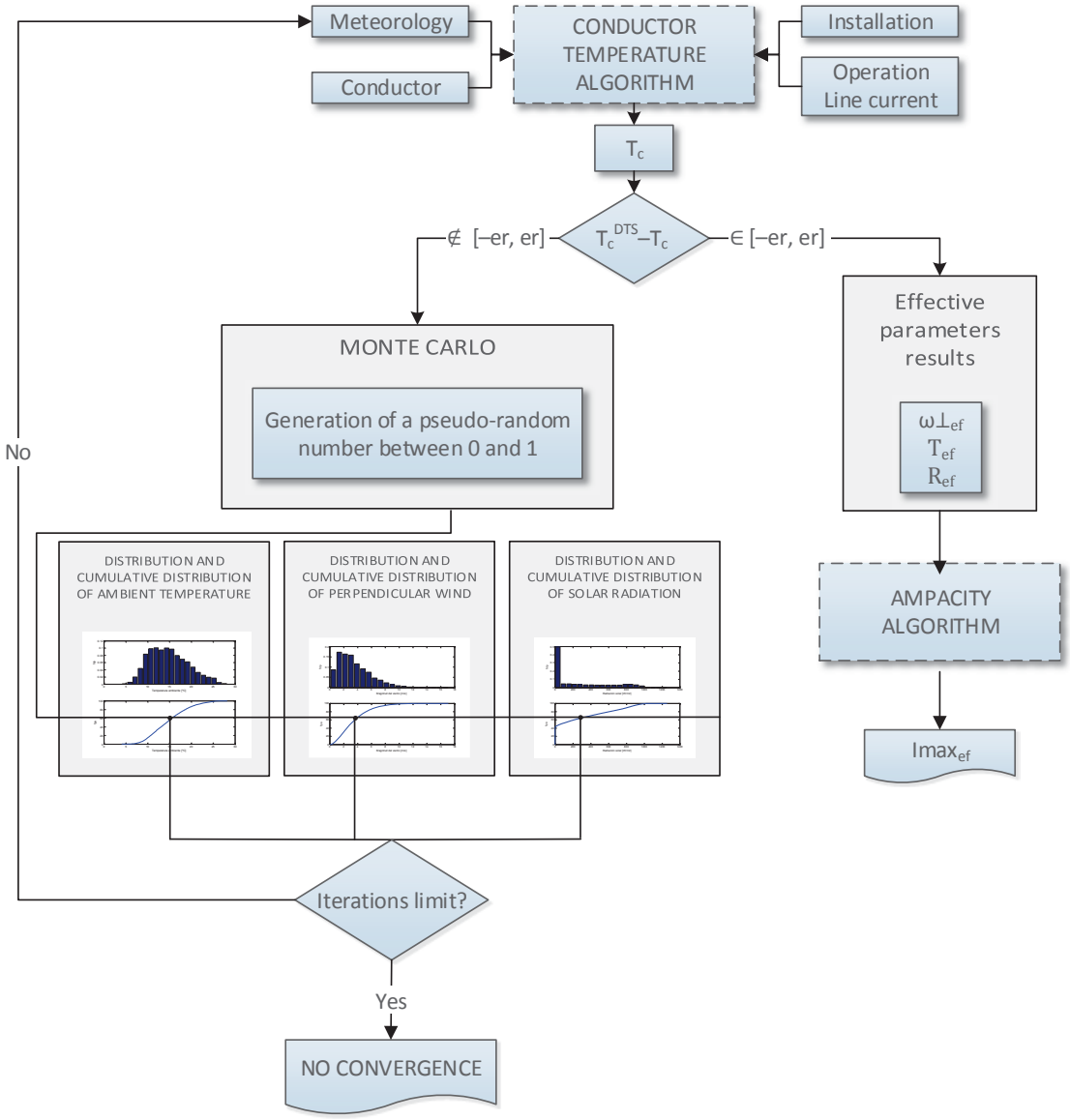

Figure 15. Monte Carlo method flow diagram.

The procedure based on Monte Carlo allows to obtain a combination of meteorological values according to the real distribution of each parameter. Thus, the effective variables are obtained in a more random way but take into account the recent past of variable values and do not depend on the order of iteration. A limit of iterations is established.

5. Results

To study the viability of each procedure, iteration or Monte Carlo, histograms of the differences between effective and measured variables, together with Root Mean Square Difference (RMSD) and correlation coefficient, are determined. It is important to obtain effective meteorological values close to measured ones, so a better method will reduce the error in temperature calculation with small variances in the set of weather conditions.

Regarding the comparison between both approaches, several parameters have to be analyzed. Not only are the simulation time period and the number of iterations essential to select the optimal approach but also the final error in the approximation of calculated and measured conductor temperature.

The histograms of differences between effective and measured variables are presented, accompanied by mean square error and correlation coefficient.

In Figure 16, it is observed that the differences between perpendicular wind and effective perpendicular wind in both procedures are similar. Approximately 90% of the cases have differences close to 0 m/s.

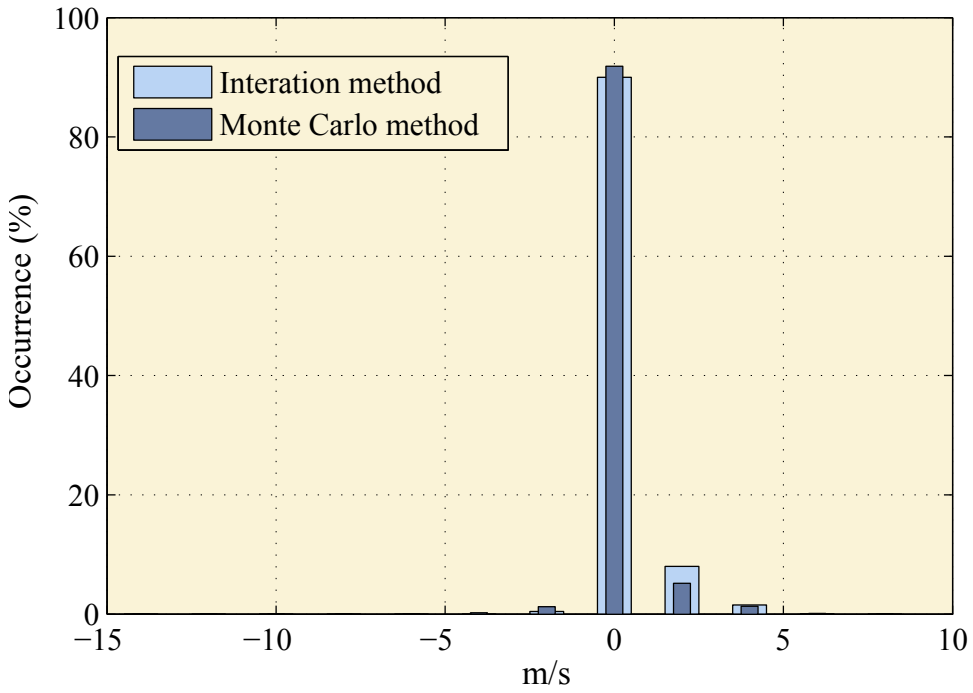

Figure 16. Differences between measured and effective perpendicular wind speed.

Regarding to ambient temperature, it is obtained similar data to wind, as shown in Figure 17. Approximately 90% of the cases have differences close to 0 °C.

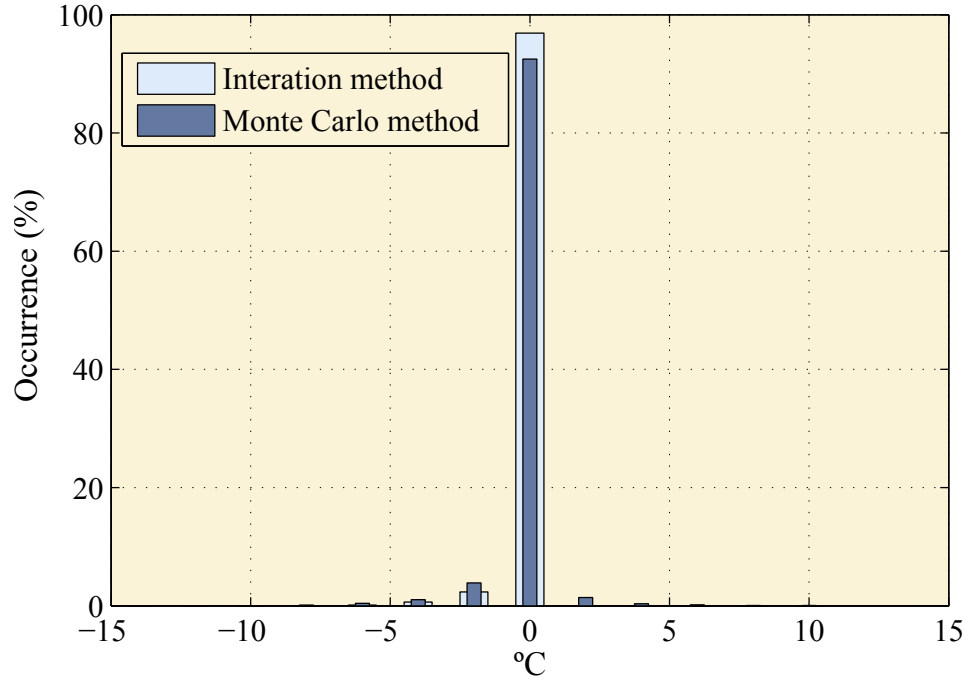

Figure 17. Differences between measured and effective ambient temperature.

In the case of solar radiation, there are more differences than in previous meteorological variables. Figure 18 shows that the iteration method obtains slightly better results than the Monte Carlo method, with differences close to 0 W/m^2 in 100% and 90% of the cases, respectively.

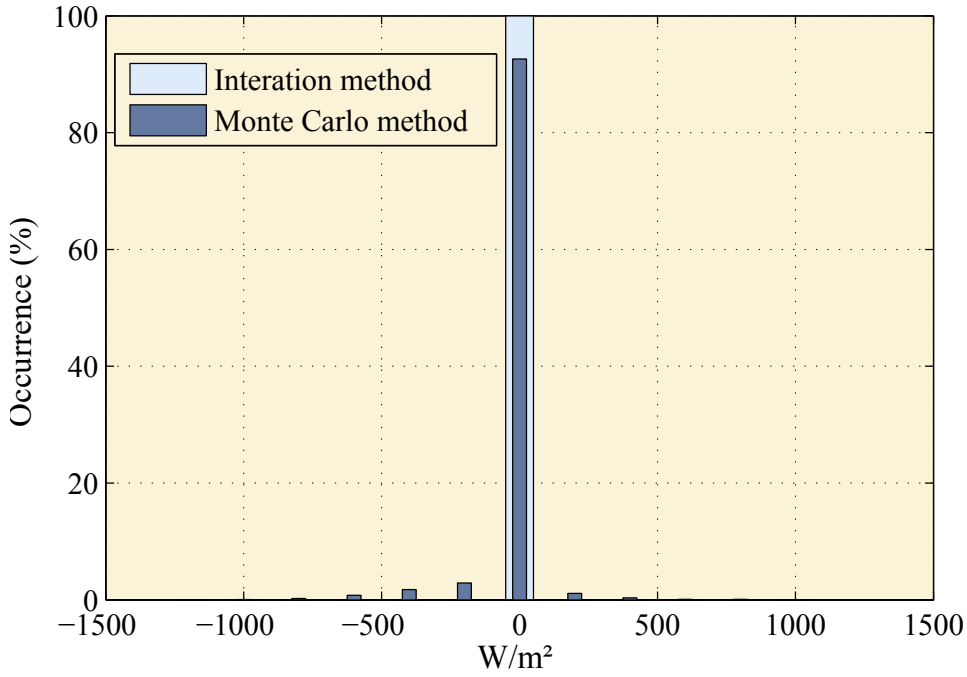

Figure 18. Differences between measured and effective solar radiation.

Although differences between meteorological variables and effective meteorological variables are similar in both methods, it is important to define which procedure obtains better results regarding conductor temperature. Figure 19 represents differences between the measured conductor temperature and the estimated one. It is observed the Monte Carlo method is a better fit in the case of conductor temperature.

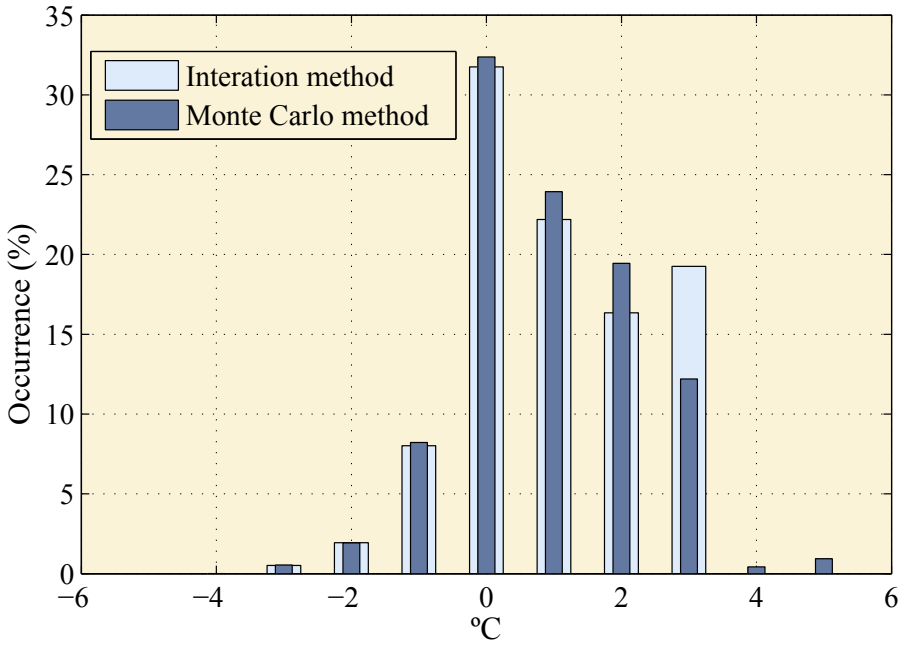

Figure 19. Differences between measured and estimated conductor temperature.

Table 1 shows the numerical results of RMSD of meteorological variables and RMSE of conductor temperature.and the correlation coefficient. In the same way as histograms, numerical results show that RMSD in perpendicular wind is lower in the Monte Carlo method, while, in ambient temperature and solar radiation, it is higher than the iteration method. Regarding conductor temperature, although the results are similar, RMSE is lower in Monte Carlo method. The latter indicates that the Monte Carlo method corrects conductor temperature slighly better than the iteration method.

Table 1. Numerical results of RMSD (for metheorological variables) and RMSE (for conductor temperature) differences between measured and estimated values.

	Perpendicular Wind (m/s)		**Ambient Temperature (°C)**		**Solar Radiation (W/m^2)**		**Conductor Temperature (°C)**	
	Iteration method	Monte Carlo method	Iteration method	Monte Carlo method	Iteration method	Monte Carlo method	Iteration method	Monte Carlo method
RMSD	0.821	0.724	0.440	0.911	0.000	104.6	1.613	1.572
Correlation	0.848	0.875	0.997	0.987	1.000	0.914	0.980	0.980

Other important parameters for the optimal selection of the procedure are the time of simulation and the iterations required in each algorithm, defined as the average number of iterations. In the case of iteration method, the simulation time was 7.36 min for 55,000 samples, with an average of iterations of 1.58. On the other hand, the Monte Carlo method simulation time was 90.20 min for 55,000 samples, with an average of iterations of 28.80.

Finally, it is possible to compare ampacity calculations with measured weather values and with effective values.

In Figure 20, it can be observed that the effective ampacity through both methods is similar but is very different from the original ampacity. Mean squared differences of around 300 A are obtained. Static ampacity of this line is aproximately 889 A, so this value represents an important difference.

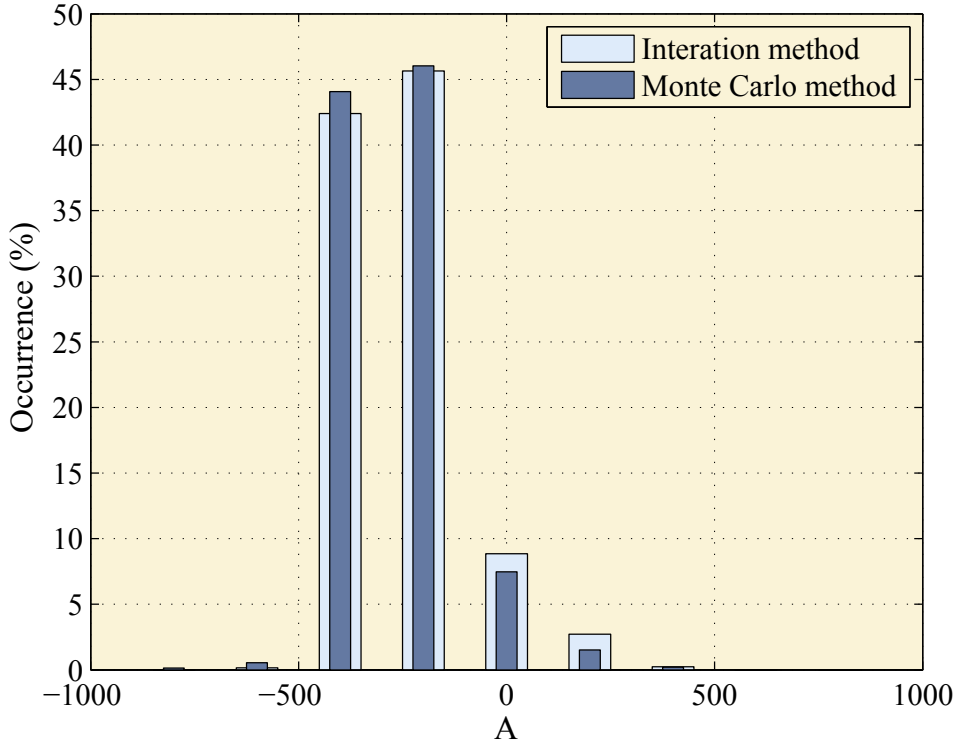

Figure 20. Differences between original ampacity calculations and effective ampacity through both methods.

6. Discussion

Focusing on the effective perpendicular wind, the difference between the measured perpendicular wind and the effective perpendicular wind is very similar. Based on this, it is concluded that with small variations of perpendicular wind is possible to correct conductor temperature errors. In addition, both iteration and Monte Carlo methods obtain similar results in the case of perpendicular wind analysis. Monte Carlo method obtains slightly better results.

In the case of effective ambient temperature, similarly to effective perpendicular wind, the differences are small in most of the cases. Therefore, with small variations of the ambient temperature, correction of the conductor temperature errors is achieved. In addition, both iteration and Monte Carlo methods obtain similar results. In contrast to perpendicular wind, iteration method obtains slightly better results.

In the case of effective solar radiation, although the differences between effective and measured values are small in most of the cases, the iteration method obtains better results than Monte Carlo method.

Finally, although the results of the calculation of conductor temperature shows that Monte Carlo method obtains more accurate results than iteration method, the difference between RMSDs is small.

Taking into account the slightly difference between the RMSDs of each method, it is important to analyze the computing workload of the methods. In this case, the results indicate that the iteration method has a simulation time period markedly lower than Monte Carlo method. In addition, the iteration method makes less iterations to obtain the corrected conductor temperature. Specifically, the Iteration method takes 8 ms per sample, while Monte Carlo method takes 98.4 ms per sample. With these results, both approaches are valid to implement in a real time system without significant delays.

7. Conclusions

An important difficulty in the integration of renewable energies is the existing limits in the power lines. Today, several techniques exist to increase the capacity of overhead lines. Due to economic, legal, and environmental constraints, the most appropriate solution is to monitor weather conditions and electric current of the overhead lines to estimate capacity and conductor temperature in real time. Distribution companies use DRM system to operate overhead lines today.

The practical application of DRM allows to find several deficiencies related to errors in T_c estimations, and consequently in I_{max}. In this paper, errors between estimated and measured conductor temperature are presented. These errors in conductor temperature and, consequently, in ampacity estimations are, in certain occasions, large, with a RMSE of 2.28 °C.

These errors encourage the design of a procedure to obtain high accuracy ampacity values. In the case of this paper, two methodologies have been tested to reduce estimation errors. Both methodologies use the variation of the weather inputs, and it is demonstrated that a reduction of the conductor temperature calculation error has been achieved and, consequently, a reduction of ampacity error. With the iteration method, a RMSE of 1.61 °C is obtained, and, with the Monte Carlo method, a RMSE of 1.57 °C. This involves a reduction of the RMSE of approximately 30%.

Once the capacity of both procedures to achieve a reduction in errors is proven, it is necessary make a decision about the most appropriate procedure. Several aspects are considered to find the optimal methodology. The more appropriate method must present the lowest errors in conductor temperature estimation with small differences between effective and measured weather values, minimum simulation time, and minimum average of iterations.

In view of the results, it can be considered that the iteration method is more suitable for the optimization of ampacity estimation. Although both methods achieve, with small variances of weather conditions, low conductor temperature errors, the iteration method

obtains better results than the Monte Carlo method. In the case of simulation time and average of iterations, iteration method simulations take 8 ms per sample and converge in an average of 1.58 iterations of the weather conditions, while, with the Monte Carlo method, simulations take 98.4 ms per sample and converge in an average of 28.8 iterations of the weather conditions.

The limitations of these procedures are based on the availability and the accuracy of real measurements of conductor temperature. Most of the DRM systems used are based only on the ampacity values without measurement of conductor temperature. In this type of system, the approaches presented in this paper are not valid to increase the accuracy. In the case of DRM systems with conductor temperature measurements, the effectiveness of the approaches of this paper will depend on the accuracy of the conductor temperature measures. In the case of DTS systems, the accuracy is higher than spot measurement systems, but they are not yet widely used due to its cost and the difficulties to install. Spot measurement sensors are widely used, but its accuracy is lower than DTS systems, and the continuity of the measurements is a problem when the location is remote. Between the two procedures, the Monte Carlo method has more limitations since, if the accuracy of the measurements is low, the algorithm could achieve the iteration limit without solution.

A future research would analyze the reduction of the limitations of these approaches, implementing an algorithm to estimate the conductor temperature measurements when a lack of measurement occurs in base on the historical values.

Author Contributions: Conceptualization, M.M. and R.M. (Raquel Martinez); methodology, M.M. and R.M. (Raquel Martinez); software, R.M. (Raquel Martinez); validation, M.M. and R.M. (Raquel Martinez); formal analysis, A.A., S.B. and A.L.; investigation, R.M. (Raquel Martinez); resources, A.A. and M.M.; data curation, R.M. (Raquel Martinez); writing—original draft preparation, A.A. and R.M. (Raquel Martinez); writing—review and editing, A.A., S.B., P.C., A.L. and R.M. (Raquel Martinez).; visualization, R.M. (Rafael Minguez); supervision, R.M. (Rafael Minguez); project administration, M.M. and R.M. (Rafael Minguez); funding acquisition, M.M. All authors have read and agreed to the published version of the manuscript.

Funding: This research was funded by the Spanish Government AND FEDER funds under the R+D initiative RETOS COLABORACIÓN 2015" with reference RETOS COLABORACIÓN RTC-2015-3795-3 and Spanish R+D initiative with reference ENE2013-42720-R.

Institutional Review Board Statement: Not applicable.

Informed Consent Statement: Not applicable.

Data Availability Statement: Restrictions apply to the availability of these data. Data was obtained from Viesgo and REE and are available from the authors with the permission of Viesgo and REE.

Acknowledgments: The authors would like to acknowledge the Spanish Government AND FEDER funds for the economical support and Viesgo and REE for technical support and data provision.

Conflicts of Interest: The authors declare no conflict of interest.

References

1. Fernandez, E.; Albizu, I.; Mazon, A.J.; Etxegarai, A.; Buigues, G.; Alberdi, R. Power line monitoring for the analysis of overhead line rating forecasting methods. *IEEE PES Power Afr.* **2016**, 119–123. [CrossRef]
2. Zhou, X.; Wang, S.; Li, T.; Cao, J.; Zou, Y.; Xiang, X. Probabilistic Ampacity Rating of 500 kV Overhead Transmission Lines in Zhejiang Province. In Proceedings of the IEEE 3rd International Conference on Integrated Circuits and Microsystems (ICICM), Shanghai, China, 24–26 November 2018; pp. 98–103.
3. Pyka, K.; Piskorski, R. DSM Based on ALS Data for Needs of Urban Space Analysis. In Proceedings of the 2018 Baltic Geodetic Congress (BGC Geomatics), Olsztyn, Poland, 21–23 June 2018; pp. 164–168.
4. Cho, J.; Kim, J.H.; Lee, H.J.; Kim, J.Y.; Song, I.K.; Choi, J.H. Development and Improvement of an Intelligent Cable Monitoring System for Underground Distribution Networks Using Distributed Temperature Sensing. *Energies* **2014**, *7*, 1076–1094. [CrossRef]
5. Holyk, C.; Liess, H.D.; Grondel, S.; Kanbach, H.; Loos, F. Simulation and measurement of the steady-state temperature in multi-core cables. *Electr. Power Syst. Res.* **2014**, *116*, 54–66. [CrossRef]

6. Marins, D.S.; Antunes, F.L.M.; Sampaio, M.V.F. Increasing Capacity of Overhead Transmission Lines—A Challenge for Brazilian Wind Farms. In Proceedings of the 6th IEEE International Energy Conference (ENERGYCon), Gammarth, Tunisia, 28 September–1 October 2020; pp. 434–438.
7. Lauria, D.; Mottola, F.; Quaia, S. Analytical Description of Overhead Transmission Lines Loadability. *Energies* **2019**, *12*, 3119. [CrossRef]
8. Erdinç, F.G.; Erdinç, O.; Yumurtacı, R.; Catalão, J.P.S. A Comprehensive Overview of Dynamic Line Rating Combined with Other Flexibility Options from an Operational Point of View. *Energies* **2020**, *13*, 6563. [CrossRef]
9. Minguez, R.; Martínez, R.; Manana, M.; Arroyo, A.;Domingo, R.; Laso, A. Dynamic management in overhead lines: A successful case of reducing restrictions in renewable energy sources integration. *Electr. Power Syst. Res.* **2019**, *173*, 135–142. [CrossRef]
10. Martinez, R.; Useros, A.; Castro, P.; Arroyo, A.; Manana, A. Distributed vs. spot temperature measurements in dynamic rating of overhead power lines. *Electr. Power Syst. Res.* **2019**, *170*, 273–276. [CrossRef]
11. Alvarez, D.L.; da Silva, F.F.; Mombello, E.E.; Bak, C.L.; Rosero, J.A. Conductor Temperature Estimation and Prediction at Thermal Transient State in Dynamic Line Rating Application. *IEEE Trans. Power Deliv.* **2018**, *33*, 2236–2245. [CrossRef]
12. Douglass, D.A.; Gentle, J.; Nguyen, H.M.; Chisholm, W.; Xu, C.; Goodwin, T.; Chen, H.; Nuthalapati, S.; Hurst, N.; Grant, I.; et al. A Review of Dynamic Thermal Line Rating Methods With Forecasting. *IEEE Trans. Power Deliv.* **2019**, *34*, 2100–2109. [CrossRef]
13. Puffer, R.; Schmale, M.; Rusek, B. Area-wide dynamic line ratings based on weather measurements. In Proceedings of the Conference on Cigre Session, Paris, France, 26–31 August 2012.
14. IEEE Standard for Calculating the Current-Temperature Relationship of Bare Overhead Conductors. *IEEE Std 738-2012 (Revision of IEEE Std 738-2006)*; IEEE: Piscataway, NJ, USA, 2012.
15. International Council on Large Electric Systems, Working Group B2.43. TB 601. *Guide for Thermal Rating Calculations of Overhead Lines*; CIGRE: Paris, France, 2014.
16. Arroyo, A.; Castro, P.; Martinez, R.; Manana, M.; Madrazo, A.; Lecuna, R.; Gonzalez, A. Comparison between IEEE and CIGRE Thermal Behaviour Standards and Measured Temperature on a 132-kV Overhead Power Line. *Energies* **2015**, *8*, 13660–13671. [CrossRef]
17. R.D. 223/2008 ITC-LAT 07: Lineas Aereas con Conductores Desnudos. 2008. Available online: https://industria.gob.es/Calidad-Industrial/seguridadindustrial/instalacionesindustriales/lineas-alta-tension/Documents/guia-itc-lat-07-rev-2.pdf (accesed on 20 February 2021).
18. Castro, P.; Arroyo, A.; Martinez, R.; Manana, M.; Domingo, R.; Laso, A.; Lecuna, R. Study of different mathematical approaches in determining the dynamic rating of overhead power lines and a comparison with real time monitoring data. *Appl. Therm. Eng.* **2017**, *111*, 95–102. [CrossRef]
19. International Council on Large Electric Systems. *Guide for Selection of Weather Parameters for Bare Overhead Conductor Ratings*; Technical Brochure 299; CIGRE: Paris, France, 2006.
20. Kosec, G.; Maksić, M.; Djurica, V. Dynamic thermal rating of power lines—Model and measurements in rainy conditions. *Int. J. Electr. Power* **2017**, *91*, 222–229. [CrossRef]
21. Laso, A.; Manana, M.; Arroyo, A.; Gonzalez, A.; Lecuna, R. A comparison of mechanical and ultrasonic anemometers for ampacity thermal rating in overhead lines. *ICREPQ* **2016**. [CrossRef]
22. Domingo, R.; Gonzalez, A.; Manana, M.; Arroyo, A.; Cavia, M.A.; del Olmo, C. Differences Using Measured and Calculated Solar Radiation in Order to Estimate the Temperature of the Conductor in Overhead Lines. *ICREPQ* **2016**. [CrossRef]
23. Morgan, V.T. *Thermal Behaviour of Electrical Conductors, Steady, Dynamic and Fault-Current Ratings*; Research Studies; John Wiley and Sons: Hoboken, NJ, USA, 1991.